PHYSICAL REVIEW B VOLUME 38, NUMBER 16 1 DECEMBER 1988

Phase lock of a weakly biased inhomogeneous long Josephson junction to an external microwave source

G. Reinisch and J. C. Fernandez
Observatoire de Nice, Boîte Postale No. 139, F-06003 Nice Cédex, France

N. Flytzanis
Department of Physics, University of Crete, Heraklio, Crete, Greece

M. Taki
Institut für Theoretische Physik, Lehrstuhl I, Universitätsstrasse 1, D-4000 Düsseldorf, Germany

S. Pnevmatikos
Research Center of Crete, P.O. Box 1527, 71110 Heraklio, Crete, Greece
(Received 25 April 1988)

Large-scale spatial inhomogeneities in a long Josephson junction, where fluxons may be trapped, allow the existence of stable periodic dynamical regimes locked to the external frequency or twice this frequency, and biased with a very weak external current. These regimes lead to an abrupt cutoff located at the bottom of the zero-field step in the corresponding current-voltage characteristics. Such an easily detectable effect strongly suggests an experimental verification of this phase-locked soliton dynamics.

I. INTRODUCTION

The phase lock of a long Josephson junction (LJJ) biased on zero-field steps (ZFS) to an external microwave field has been extensively studied.[1-4] Indeed, shuttling fluxons (quanta of magnetic flux) generate a periodic leakage of energy resulting in emission of a very narrow linewidth of electromagnetic radiation at the shuttling frequency (and its harmonics) at either end of the LJJ.[5-11] Therefore, they can be considered as potentially interesting parametric oscillators, provided that the output power of such a LJJ oscillator is not too low. Unfortunately, in the case of a single device the output power P_0 is of order of only a few picowatts.

Hence, the idea of building a series array of n phase-locked LJJ's appears as a natural way to overcome this serious limitation for practical applications, since it is known that the total emitted power grows as n^2P_0, while the linewidth decreases as n^{-1}.[12] Recently, eight LJJ's locked together exhibited a 15 dB amplification while the predicted value is 17 dB. The corresponding emitted power exceeded 10 nW.[13]

The usual experimental procedure involves dc-biasing the coupled junctions, whose coherent locking, due to their mutual exchange of electromagnetic radiation, leads to the observation of superradiant states.[3,4,14] The dc biasing may be the same for all junctions (series array) or independent for each one. The interest of this last bias configuration is that it allows frequency adjustment. For example in the case of a two-junction device, both frequencies may be adjusted in order to detect the coherence between the two LJJ's in their mutual exchange of photons.[4]

Moreover, the I-V current-voltage characteristics of the (array of) junctions is one natural way to compare the physical states corresponding to the locked and the unlocked regime from an experimental point of view; by looking at the I-V characteristics of a LJJ biased on the second ZFS with and without an external microwave signal generating a 50 MHz interval of coherence, Cirillo and Lloyd[4] concluded from the very small differences between the shapes of the two characteristics that only a tiny amount of radiation power was needed in order to lock the junction over a frequency interval of roughly 0.7% of the LJJ oscillation frequency.

Hence, the dc biasing of the array of coupled junctions is convenient, from an experimental point of view, for detecting basic properties of the locking processes. Is it necessary from a theoretical point of view? In other words, do phase-locked regimes exist where the external dc bias is either zero or very weak (i.e., a few percent of the critical current)? This paper addresses this question.

If the answer is affirmative, the corresponding I-V characteristics should look like a slightly distorted one for "high" dc values (typically more than one tenth of the critical current), with an abrupt vertical cutoff at the voltage values corresponding to the phase-locked regimes at small dc bias (see Fig. 1).

The main technical question that arises it the very possibility of obtaining a fluxon in such regimes. In absence of any inhomogeneity in the LJJ able to trap the fluxon, a fluxon in unstable with respect to a zero-bias state (it is attracted toward either end of the LJJ and is annihilated there because of the presence of the damping). One possible way to overcome this difficulty could be to reach the zero-dc states starting from the intermediate part of the I-V characteristics corresponding to roughly half of the critical current in the chosen ZFS, and then decreasing the bias.

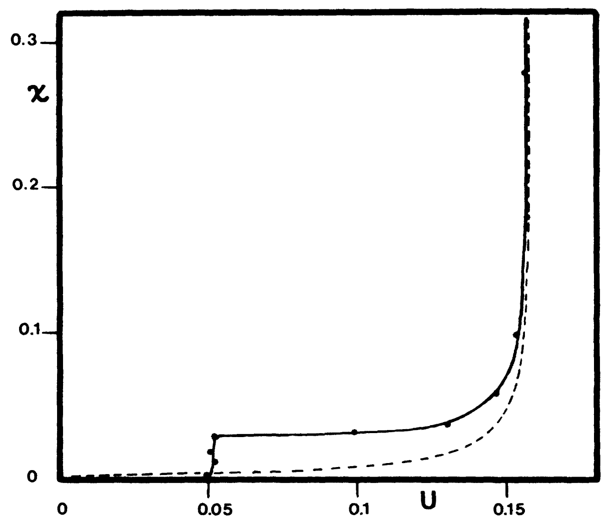

FIG. 1. Current-voltage characteristic corresponding to the following choice of parameters [see definitions in Eq. (2)]: $L=40$, $a=20$, $b=0.095$, $\varepsilon=0.1$, $\Omega=0.055$, $\beta_c=10^4$. The voltage U, defined by Eqs. (12), was found fairly uniform inside of the junction, for $-10\le Y\le 10$. The fluctuations within this region were less than 10^{-3}. Therefore the value U plotted here is obtained by Eq. (12a) and averaged over this central area. Actually, the voltage value (12a) found at both ends $Y=\pm 20$ of the LJJ is approximately half the above value U. The dashed curve is the ZFS; $\chi=(4\alpha/\pi)(U/\lambda)[1-U^2/\lambda^2]^{-1/2}$ where $\lambda=0.157$ is the scaling factor allowing a comparison of $\chi(U)$ with the corresponding unperturbed ($a=b=\varepsilon=\alpha=0$) ZFS.

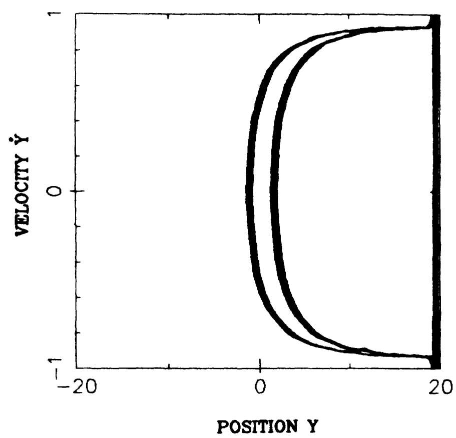

FIG. 2. The phase-plane trajectory of an initial antikink obtained by a direct numerical simulation of the PDE (1) where: $L=40$, $\varepsilon=0.2$, $\Omega=0.06$, $\beta_c=10^4$. This trajectory—displaying a quasi-periodic bouncing of the antikink against the right end of the LJJ at the frequency 2Ω, alternatively following the internal and to the external branch—is obtained by plotting the soliton velocity $\dot{Y}$ vs the position Y for the time values ranging from $t=500$ to $t=1500$.

We have first performed numerical simulations using the following (reduced) partial differential equation (PDE), which is known to describe in an acceptable way the physics of the damped, driven fluxon dynamics inside of an homogeneous LJJ:[11,15,16]

$$\Phi_{tt}-\Phi_{xx}+\sin\Phi=\varepsilon\cos(\Omega t+\theta)-\frac{1}{\sqrt{\beta_c}}\Phi_t\ , \tag{1a}$$

with

$$\Phi_x(\pm L/2)=0\ , \tag{1b}$$

where the external microwave field amplitude ε is in units of the maximum Josephson current density, the corresponding radiation frequency Ω is in units of the LJJ plasma frequency, β_c is the McCumber number, the time t and the position x—as well as the LJJ length L—are respectively given in units of the reciprocal of the plasma frequency and in units of the Josephson penetration depth. We have not yet been able to obtain stable asymptotic fluxon dynamical regimes coherently locked to (harmonics of) the external field. Although there are indications that such regimes may develop (see *Note added in proof*), the ranges of the parameters $\varepsilon,\Omega,\theta,\beta_c,L$, are sharply peaked on particular values. These values allow an unstable regime phase-locked to 2Ω (if one considers the frequency of the fluxon bouncing against the LJJ end). In Fig. 2, the thick trajectories obtained by a direct numerical simulation of Eq. (1) display a slowly changing periodic bouncing of the fluxon against the right junction end, between the normalized time values 500 and 1500. The thickness of the lines means a slow detuning between the fluxon oscillations and the periodic external field, leading to instability of this phase-locked regime.

Quite different is the situation if a large scale (compared to the Josephson penetration depth) inhomogeneity is present in the LJJ. More precisely, introducing a "Josephson-current-density potential well" in the PDE [Eq. (1)] (as well as the very weak constant bias),[17] one obtains

$$\Phi_{tt}-\Phi_{xx}+[1+\tfrac{1}{4}V(x)]\sin\Phi=\chi+\varepsilon\cos(\Omega t+\theta)-\frac{1}{\sqrt{\beta_c}}\Phi_t\ , \tag{2a}$$

where we assume

$$V(x)=a[1-\operatorname{sech}(bx)],\ L^{-1}\ll b\ll 1,\ \text{and}\ \chi\ll 1\ . \tag{2b}$$

This leads to a clear asymptotic phase-locking to half of the external frequency Ω of an initial (anti)fluxon

$$\Phi(x,0)=4\tan^{-1}\exp(-\sigma\gamma x)\ , \tag{2c}$$

$$\gamma=(1-v^2)^{-1/2}\ , \tag{2d}$$

$$\text{kink: } \sigma=-1;\ \text{antikink: } \sigma=+1\ , \tag{2e}$$

located, say, at the middle of the LJJ (or, equivalently at the bottom of the potential well), with almost any initial velocity v satisfying

$$0 \leq v < 1 \ . \tag{2f}$$

The locking domain in the $\{\Omega, \chi\}$ plane is approximately $0.03 \leq \Omega \leq 0.07$ versus $0 \leq \chi \leq 0.03$. There is no doubt that phase-locked soliton dynamics to $\frac{1}{2}\Omega$ exist for very weak external bias. A typical corresponding phase-locked cycle in the fluxon phase space $\{Y, \dot{Y}\}$, where Y is the fluxon position defined as $\Phi_x(Y(t),t)$=maximum and $\dot{Y}=(-\Phi_t/\Phi_x)_{x=Y}$ is the flux velocity, is shown on Fig. 3. The thick dotted line indicates the (asymptotic) trajectory of the fluxon performed within one period $T=2\pi\Omega^{-1}$ of the external periodic field, while the thin dotted line shows the trajectory corresponding to the next period. Therefore, the Poincaré mapping of such a phase-locked cycle is reduced to a coupled of points. The labeling of the cycle displayed in Fig. 3 allows understanding of the resonant process which leads to phase locking. Indeed, Fig. 4 sketches the driving force that the fluxon actually experiences (note that a reflection at either end of the LJJ changes the sign of σ and, hence, the sign of the driving force, since the fluxon here is basically Newtonian.[17,18] Figure 5 illustrates the corresponding trajectory in the trapping potential. The process is resonant because the driving force is always synchronized with the fluxon motion.

II. A THEORETICAL MODEL

The theory which explains these results makes an extensive use of the collective-coordinate description of reference.[17] Indeed, it was shown that a sine-Gordon SG (anti)kink trapped in a (harmonic) potential may be described by a single degree of freedom, namely the soliton position $Y(t)$

$$\Phi_S(x,t)=4\tan^{-1}\exp\{-\sigma k[x-Y(t)]\} \ , \tag{3a}$$

where

$$k=k[Y,\dot{Y}]=\left\{\frac{[1+\frac{1}{4}V(Y)]}{(1-\dot{Y}^2)}\right\}^{1/2} \ . \tag{3b}$$

The corresponding equation of motion of the quasisoliton (3) is obtained by means of the classical Hamiltonian theory in the case $\beta_c=\infty$, and reads

$$k\dot{P}=-\frac{dV}{dY}+2\pi\sigma k[\varepsilon\cos(\Omega t+\theta)+\chi] \ , \tag{4a}$$

where P is the canonical momentum:

$$P=8k\dot{Y} \ . \tag{4b}$$

Clearly, the soliton dynamics is Newtonian when relativistic effects are discarded, i.e., when $k \sim 1$. Adding the dissipative term $-\beta_c^{-1/2}\Phi_t$ in the PDE (2a) results in the

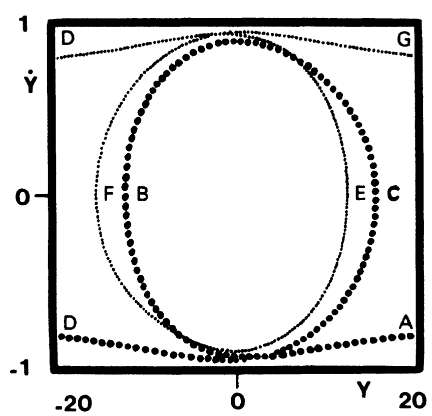

FIG. 3. The asymptotic phase-locked cycle obtained either by a direct numerical simulation of the PDE (2) or by the numerical solution of the ODE system (5,7,10,11), where $L=40$, $a=20$, $b=0.095$, $\varepsilon=0.1$, $\Omega=0.045$, $\beta_c=10^4$, $\chi=0.01$. The cycle was obtained for $15\,000 \leq t \leq 20\,000$. The trajectory $ABCD$ is described during one period of the external field, while the trajectory $DEFG$ is described during the next period.

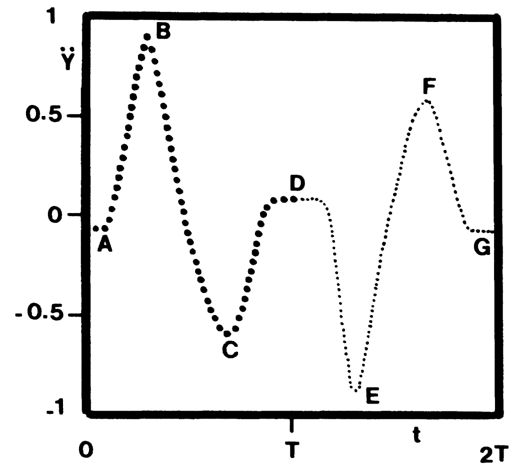

FIG. 4. The fluxon driving force, defined as the rhs of Eq. (5) vs time, corresponding to the trajectory $ABCDEFG$ displayed on Fig. 3.

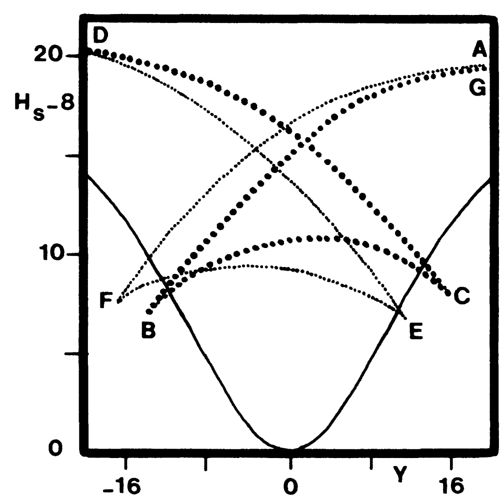

FIG. 5. The trajectory $ABCDEFG$ of Fig. 3, displayed in the following energy diagram: soliton energy H_S [minus the rest energy equal to 8: cf., Eq. (9)] vs soliton position Y. The continuous line displays the potential well (2b) where $a=20$ and $b=0.095$. Here $L=40$.

dissipative term $-\beta_c^{-1/2}kP$ in the rhs of (4a), and leads to the final equation of motion of the (anti)fluxon

$$\ddot{Y}=\frac{-1}{8k^2}\frac{dV}{dY}+\frac{1-\dot{Y}^2}{8k}\{2\pi\sigma[\mathcal{X}+\varepsilon\cos(\Omega t+\theta)]-8\beta_c^{-1/2}k\dot{Y}\}\ , \tag{5}$$

where k is given by (3b). Note that, assuming $\varepsilon=\mathcal{X}=\beta_c^{-1/2}=0$ leads to

$$\ddot{Y}=-\tfrac{1}{2}(1-\dot{Y}^2)\frac{d}{dY}\ln[1+\tfrac{1}{4}V(Y)]\ , \tag{6}$$

which emphasizes the nonlinear "potential-saturation-effect" at high-energy values, due to the log function: for instance, if $V(Y)=\kappa Y^2$, the force on the soliton is proportional to $-Y^{-1}$ for large values of Y and small velocities.

Equation (5) is a second-order ordinary differential equation (ODE) which describes the dynamics of a periodically driven and damped nonlinear oscillator. Its configuration space $\{Y,\dot{Y},t\}$ may therefore exhibit resonances and chaotic regions. Actually, the cycle displayed in Fig. 3 is an example of such a resonance in which the frequency of the cycle and the frequency of the external field are in a simple commensurate ratio, namely $\frac{1}{2}$.

Due to the non-Hamiltonian dynamics described by the original PDE (2a) ($\beta_c<+\infty$), the collision between a soliton and an antisoliton—or, equivalently, the reflection of a (anti)soliton at either end of the LJJ where the square of the plasma frequency is approximated to $1+\frac{1}{4}a$ [cf. Eq. (2b)]—is inelastic and displays both a "phase shift:"

$$Y^+=\mathrm{sgn}(Y)\left[\frac{L}{2}+2\left[\frac{(1-\dot{Y}^2)}{1+\frac{1}{4}a}\right]^{1/2}\ln|\dot{Y}|\right] \tag{7}$$

(where Y^+ means the value of Y immediately after the reflection at $Y=\pm L/2$), and an energy loss approximately equal to

$$\Delta H=\frac{2\pi^2}{[\beta_c(1+\frac{1}{4}a)]^{1/2}}\ , \tag{8}$$

for a single soliton having a velocity close to one (which is being checked *a posteriori*).[16,19–21] Assuming that the value of the potential in the neighborhood of either end of the junction is almost constant and equal to a [cf. (2b)], the soliton energy in these regions is

$$H_S\,|_{\,|Y|\lesssim L/2}=8\left[\frac{1+\frac{1}{4}a}{1-\dot{Y}^2}\right]^{1/2}\ . \tag{9}$$

The soliton annihilation occurs for low velocities when the kinetic energy $4\dot{Y}^2(1+1/4a)^{1/2}$ is less than the energy loss ΔH. We obtain the following threshold reflection velocity:

$$\dot{Y}_{\min}=\frac{\pi\beta_c^{-1/4}}{[2(1+\frac{1}{4}a)]^{1/2}}\ . \tag{10}$$

Moreover, differentiating (9) with respect to $\dot{Y}$ and equating the result to ΔH given by Eq. (8) leads to the following expression of the change of the soliton velocity at the reflection

$$\dot{Y}^+=[-\dot{Y}]_{Y=\pm L/2}\left[1-\frac{\pi^2(1-\dot{Y}^2)^{3/2}}{4\sqrt{\beta_c}(1+\frac{1}{4}a)\dot{Y}^2}\right]\ . \tag{11}$$

Equations (7), (10), and (11) model the inelastic boundary conditions of the soliton PDE Eqs. (1b) and (2), when the soliton dynamics is approximated by the ODE Eq. (5). The numerical simulations of these PDE and ODE equations are in excellent agreement and, for instance, the asymptotic cycle shown on Fig. 3 is recovered up to a high accuracy by the numerical solution of the ODE system (5), (7), (10), and (11) (see Fig. 6). Note that the reflections occur for soliton velocities close to one, in agreement with approximation (8).

III. ADDITIONAL COMMENTS

(1) In the "locking region," all cycles are not locked to 2Ω. Actually, some are locked to Ω, and consist in a single loop inside of the potential well, followed by a straight return [cf. Figs. 7(b) and 7(c), for $\mathcal{X}=0.02$ and, respectively, $\Omega=0.035$ and $\Omega=0.04$]. Moreover, for a given value of the (small) bias, $\mathcal{X}$, the increase of the driving field frequency Ω allows a transition from a Ω-locking regime (simple loop) to a $\frac{1}{2}\Omega$-locking regime (double loop); see Figs. 7(a)–7(f). Clearly, these single-looped cycles are not as stable as the double-looped ones (consider for instance the qualitative arguments sketched by Figs. 3–5). This may be the reason for the relatively small number of such cycles found in the locking domain of the phase space.

(2) When the external bias $\mathcal{X}$ exceeds a certain "high" value—typically $\mathcal{X}>0.05$ for the range of the parameters which are considered in the present paper—the locking to the periodic field disappears; there is no loop at all in the configuration space and the fluxon dynamics become trivial (perturbed) shuttling dynamics. More complicated phenomena may then occur if geometrical resonances are

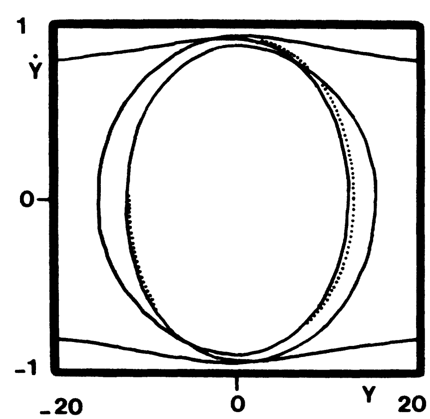

FIG. 6. The comparison between the numerical solution of the ODE system (5,7,10,11) (solid line) and the PDE system (1b,2) (dotted line) for the same parameters as in Fig. 3.

then made possible between the shuttling frequency—basically determined by $\mathcal{X}$ and β_c—and the external periodic field frequency. However, such phenomena require higher bias values and are out of the scope of the present paper.

(3) Comments one and two both lead to a truncated ZFS at low bias values, which is illustrated on Fig. 1 for a typical choice of the parameters ($\beta_c=10^4$, $\Omega=0.055$, $\varepsilon=0.1$, $a=20$, $b=0.095$, and $L=40$). Since the original PDE soliton dynamics is correctly modeled by the ODE system (3,5,7,10,11), the averaged voltage U at a given point $X=X^*$ is calculated according to the following formulas:

$$U\,|_{Y=X^*}=\overline{\Phi}_t\,|_{X=X^*}$$
$$=\frac{2}{T}\int_0^T \operatorname{sech}[\xi(X^*)]\left[\frac{\dot{k}}{k}\xi(X^*)-\sigma k\dot{Y}\right]dt\ , \tag{12a}$$

where Φ is given by (3), and

$$\xi(X^*)=\sigma k(X^*-Y)\ , \tag{12b}$$

$$\frac{\dot{k}}{k}=\dot{Y}\left[\frac{\ddot{Y}}{1-\dot{Y}^2}+\frac{1}{8}\frac{V_Y}{1+\frac{1}{4}V}\right]\ , \tag{12c}$$

while $\ddot{Y}$ is given by Eq. (5) and $V_Y=dV/dY=ab\,\operatorname{sech}^2(bY)\sinh(bY)$. The results vary according to the choice of X^*. Then a spatial average is made between characteristic values corresponding to several X^*.

The transition to a chaotic unlocked regime when the system just leaves the locking domain is illustrated on Fig. 8. It seems to occur via a period-doubling cascade-bifurcation process. This important result, which has to be compared with those of Refs. 22 and 23, is only preliminary and will be detailed in a next paper.[24]

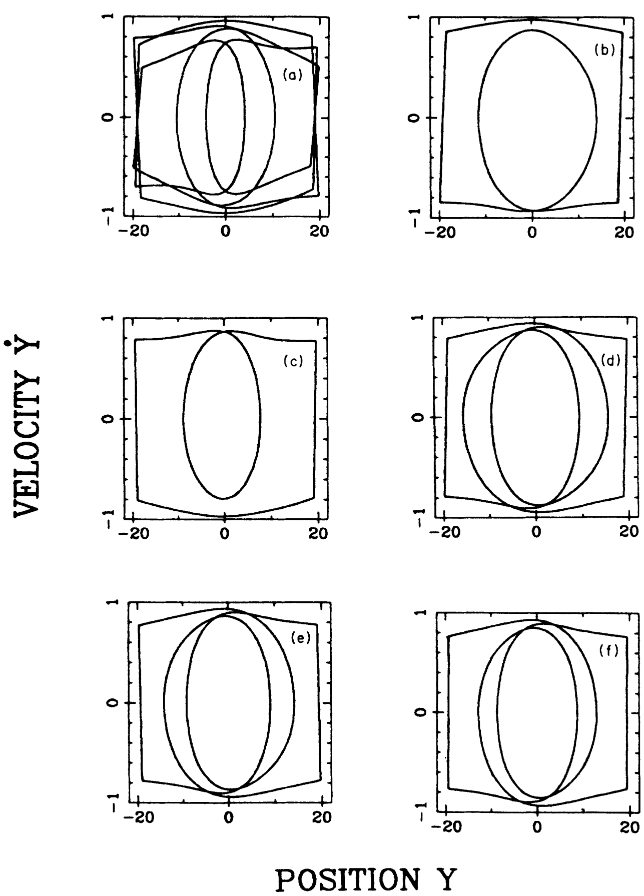

FIG. 7. A sequence of limit cycles for fixed bias field $\mathcal{X}$ and increasing external frequency Ω, which are phase locked either to $\frac{1}{2}\Omega$ [(a),(d),(e),(f)] or to Ω[(b),(c)]. Note the peculiar sophisticated cycle displayed on (a). The parameters are $L=40$, $a=20$, $b=0.095$, $\varepsilon=0.1$, $\beta_c=10^4$, $\mathcal{X}=0.02$. (a)–(f), respectively, correspond to the values of Ω equal to 0.03, 0.035, 0.04, 0.045, 0.047, 0.049, 0.051. All cycles were obtained by the numerical simulation of the ODE system (5,7,10,11) between time values 17 000 and 20 000. These trajectories were checked by direct numerical simulations of the PDE system (1b,2).

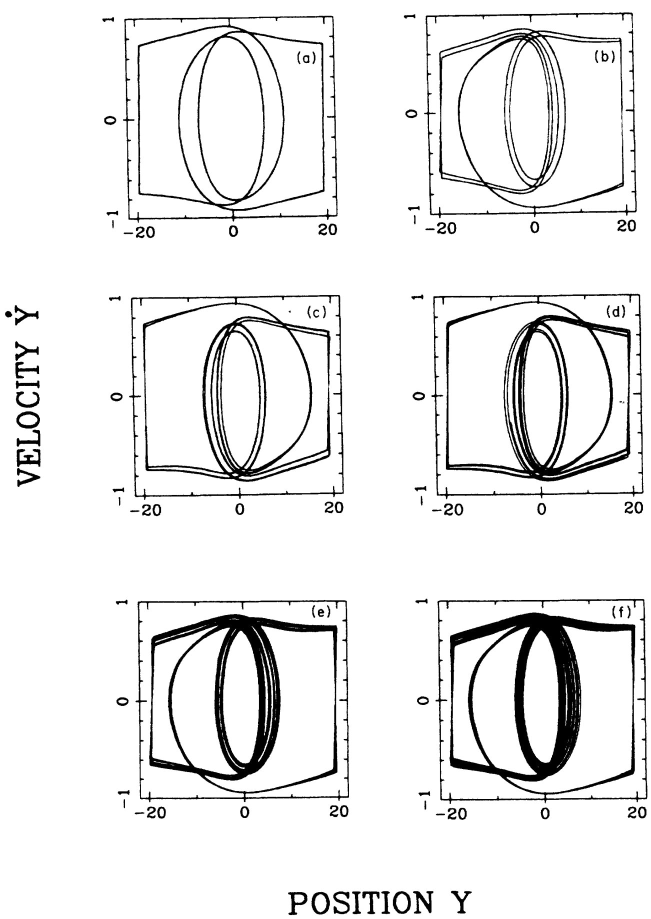

FIG. 8. A sequence of limit cycles obtained by Fernandez, Goupil, and Reinisch (Ref. 24) from the numerical solution of the ODE system (5,7,10,11) for fixed external field frequency Ω and increasing bias values $\mathcal{X}$, clearly displaying a period-doubling route to chaos. The parameters are $L=40$, $a=20$, $b=0.095$, $\varepsilon=0.1$, $\beta_c=10^4$, $\Omega=0.055$. (a)–(f), respectively, correspond to values of $\mathcal{X}$ equal to 0.023, 0.027, 0.0271, 0.0272, 0.0273, 0.0274. These trajectories were checked by direct numerical simulations of the PDE system (1b,2). A fully chaotic state, described by a strange attractor in the phase space $\{\dot{Y},Y\}$, is obtained for $\mathcal{X}=0.03$.

Note added in proof. By considering an ac bias current which is spatially modulated, according to $\varepsilon = \varepsilon(x) = \varepsilon_0 \cos\kappa x$, Fernandez, Grauer, and Reinisch have obtained a single *stable* "*c* cycle" similar to the trajectory displayed in Fig. 2. The parameter κ was chosen according to the resonant condition for the external microwave field: $\kappa = \Omega$, while the length L was equal to half of the wavelength $2\pi/\kappa$. All other parameters were as indicated in Fig. 2.

ACKNOWLEDGMENTS

This work was financially supported by the EEC (European Economic Community) Contract No. ST2-0267-J-C. The authors wish to thank N. F. Pedersen and M. J. Goupil for interesting discussions and careful reading of the manuscript.

[1]T. F. Finnegan and S. Wahlsten, Appl. Phys. Lett. **21**, 541 (1972).
[2]M. Cirillo, J. Appl. Phys. **58**, 3217 (1985).
[3]M. Cirillo, J. Appl. Phys. **60**, 338 (1986).
[4]M. Cirillo and F. L. Lloyd, J. Appl. Phys. **61**, 2581 (1987).
[5]T. A. Fulton and L. N. Dunkleberger, Appl. Phys. Lett. **22**, 232 (1973).
[6]B. Dueholm, O. A. Levring, J. Mygind, N. F. Pedersen, O. H. Soerensen, and M. Cirillo, Phys. Rev. Lett. **46**, 1299 (1981).
[7]E. Joergensen, V. P. Koshelets, R. Monaco, J. Mygind, M. R. Samuelsen, and M. Salerno, Phys. Rev. Lett. **49**, 1093 (1982).
[8]Y. S. Kivshar and B. A. Malomed, Phys. Lett. **118A**, 85 (1986).
[9]O. A. Levring, M. Cirillo, B. Dueholm, E. Joergensen, J. Mygind, O. H. Olsen, N. F. Pedersen, M. R. Samuelsen, and O. H. Soerensen, Physica Scripta **25**, 810 (1982).
[10]O. H. Olsen, N. F. Pedersen, M. R. Samuelsen, H. Svensmark, and D. Welner, Phys. Rev. B **33**, 168 (1986).
[11]A. Barone and G. Paterno, *Physics and Applications of the Josephson Effect* (Wiley, New York, 1982).
[12]R. Bonifacio, Phys. Lett. **101A**, 427 (1984).
[13]R. Monaco, S. Pagano, and G. Costabile (unpublished).
[14]M. Cirillo, S. Pace, and S. Pagano, Phys. Lett. **125A**, 20 (1987).
[15]N. F. Pedersen, in *Advances in Superconductivity,* edited by B. Deaver and J. Ruvolds (Plenum, New York, 1982).
[16]N. F. Pedersen, in *Solitons,* edited by S. E. Trullinger, V. E. Zakharov, and V. L. Pokrovsky (Elsevier, New York, 1986).
[17]J. C. Fernandez, M. J. Goupil, O. Legrand, and G. Reinisch, Phys. Rev. B **34**, 6207 (1986).
[18]J. C. Fernandez, J. P. Leon, and G. Reinisch, Phys. Rev. B **27**, 5817 (1983).
[19]N. F. Pedersen, M. R. Samuelsen, and D. Welner, Phys. Rev. B **30**, 4057 (1984).
[20]D. Welner, Ph.D. thesis, Lyngby University (1985).
[21]D. W. McLaughlin and A. C. Scott, Phys. Rev. A **18**, 1652 (1978).
[22]K. Fukushima and T. Yamada, J. Phys. Soc. Jpn. **55**, 2581 (1986).
[23]K. Fukushima and T. Yamada, J. Phys. Soc. Jpn. **56**, 467 (1987).
[24]J. C. Fernandez, M. J. Goupil, and G. Reinisch (unpublished).